International Journal of Innovative Computing, Information and Control
Volume **9**, Number **11**, November **2013**

 ISSN 1349-4198
pp. 4447–4457

COMPARISONS OF SENSOR GEOMETRIES FOR ELECTRICAL CAPACITANCE VOLUME TOMOGRAPHY

Marlin Ramadhan Baidillah[1,2], Muhammad Mukhlisin[1,3] and Warsito Purwo Taruno[2,4]

[1]Department of Civil and Structural Engineering
Universiti Kebangsaan Malaysia
Bangi, Selangor 43600, Malaysia
marlinrb@eng.ukm.my; mmukhlis2@yahoo.com

[2]CTECH Laboratories
Edwar Technology Co., Ltd.
Alam Sutera, Tangerang Selatan, Indonesia

[3]Department of Civil Engineering
Polytechnic Negeri Semarang
Jl. Prof. Sudarto, SH, Tembalang, Semarang 50275, Indonesia

[4]Department of Physics
University of Indonesia
Jakarta, Indonesia

Received June 2012; revised October 2012

Abstract. *Proper electrode design to generate uniform sensitivity distribution is crucial for robust volumetric imaging based on electrical capacitance volume tomography (ECVT). Certain designs commonly used in electrical capacitance tomography (ECT), such as rectangular electrodes, form so-called "dead zones", i.e., regions with no variation in sensitivity among capacitance measurements between electrode pairs, making it impossible to differentiate the permittivity within a given region. For robust volumetric imaging, an electrode design that generates a sensitivity distribution that provides variation along all three directions with equal strength is required. In this work, several ECVT sensor electrode designs with various geometrical shapes were considered, and their performance in volumetric image reconstruction was evaluated based on experimental data. The electrode designs included regular square, triangular, trapezoidal and hexagonal shapes based on a 32-electrode capacitance sensor arranged with 8 electrodes along the radial direction and 4 electrodes along the axial direction. From the reconstruction results using experimental data, the horizontally aligned hexagonal electrode showed the best consistency in terms of the shape of the object that was reconstructed.*
Keywords: ECVT, ECT, Volumetric imaging, 3D capacitive imaging, Sensor design

1. **Introduction.** Electrical capacitance volume tomography (ECVT) has allowed capacitance tomography to play an important role after being successfully applied in multiphase systems such as velocity measurement of multiphase flows [1], fluidized bed systems [2-5], gas-liquid and gas-liquid-solid systems [6], and soil-water systems [7]. Moreover, Wang et al. have published a review of ECVT designs and applications and reported that ECVT has a real-time 3D feature, can be applied in complex geometries, is inexpensive, and features low-profile sensors, which give rise to other imaging technologies [8]. Gaining acceptance as a tool for the direct analysis of multiphase systems has made ECVT become more widely used as a robust non-invasive imaging instrument.

ECVT can reconstruct volumetric data using a 3D capacitance sensor design [9]. It is the improvement of Electrical Capacitance Tomography (ECT) which can reconstruct in quasi-3D. As a capacitance tomography technique that features a nonlinear relationship among the interested and measured parameters, ECVT and ECT have a shortcoming regarding image resolution. A solution formulated during the early development of ECVT was a new robust image reconstruction algorithm called Neural Network-Multicriterion Optimization Image Reconstruction Technique (NN-MOIRT). This volume image reconstruction technique tries to overcome the so-called "sensitivity-caused artefacts" that occur in several image reconstruction algorithms. NN-MOIRT provides a 3D sensitivity matrix and additional network constraints, including a 3D-to-2D image matching function. Some studies have proven that NN-MOIRT enhances the accuracy of image reconstruction algorithms [9,10].

Another crucial aspect in the development of ECVT is the capacitance sensor. It is known that 2D ECT exhibits a fringing effect that blurs the reconstructed image. This is due to the limited length of the sensor, which distorts electric field lines [11]. Although regarded as an undesired component in 2D ECT, the sensor in ECVT is considered useful instead of limiting. A 3D capacitance sensor functions based on the fringing effect and consists of sensors that are stacked into layers. It is employed to produce an electric field distribution that has a uniform variation along both the axial and radial directions. The electric distribution is directly related to the sensitivity distribution. Moreover, the accuracy of the reconstructed image also depends on the variation in the sensitivity distribution.

Recently, ECVT sensors have adopted rectangular designs, which are commonly used in ECT. Although these sensors have successfully enhanced the accuracy of reconstructed images due to the use of NN-MOIRT, the designed electrodes suffer from so-called "dead zones", i.e., regions with no variation in sensitivity among capacitance measurements between electrode pairs, making it impossible to differentiate the permittivity within a given region. Electrode designs that can generate uniform sensitivity distribution along all three directions with equal strength are crucial for robust volumetric imaging based on ECVT. Therefore, the key issue in 3D capacitance sensors design is the capability to generate a uniform electric field distribution. The design of electrode sensors considers not only the sensor shape but also the configurations and number of channels. These sensors play an important role in both 2D ECT and 3D ECVT measurements [8].

In the earlier study, Warsito et al. have analyzed several designs of ECVT sensor in order to extract the performance whether in sensitivity strength or sensitivity variation [9]. The designs of ECVT that analyzed are single-plane triangular, triple-plane rectangular, twin-plane rectangular, twin-plane triangular and twin-plane trapezoidal. It was concluded that the triple-plane rectangular sensor makes the reconstructed image be better than other designs. Due to the nonlinearity of the electric field, there is called the fringing effect which allowed us to measure the capacitance pair between the adjacent electrode. Thus, the sensor can be used without restricted at only one design. Therefore, the possibility of another design that is better than a triple-plane rectangular sensor is possible.

To enhance the accuracy of image resolution, this study was conducted with the specific aim of developing a new electrode. In this work, several electrode designs featuring various geometrical shapes for the ECVT sensor were considered. These included regular-square, triangular, trapezoidal and hexagonal shapes based on a 32-electrode capacitance sensor arranged with 8 electrodes along the radial direction and 4 electrodes along the axial direction. The performance of each design with respect to volumetric image reconstruction was evaluated based on the experimental study.

2. **Principle of Electrical Capacitance Volume Tomography.** ECVT tries to predict the permittivity distribution of an unknown medium by measuring the capacitance data. Capacitance data are acquired by attaching an ECVT sensor consisting of a number of electrodes around a vessel. Generally, the vessels used are cylindrical in shape. An ECVT system requires three main components, as shown in Figure 1.

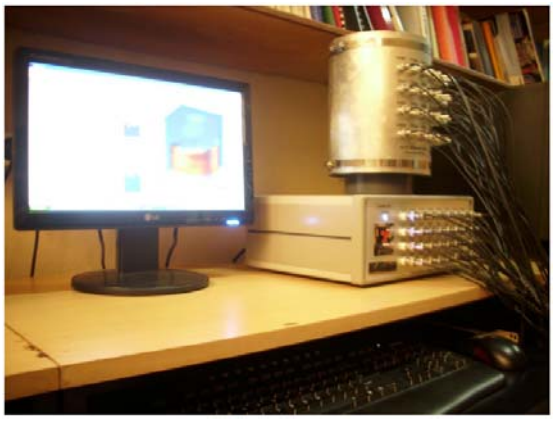

FIGURE 1. Schematic of ECVT system

2.1. **Principle of capacitance measurement.** ECVT measurement is performed in two stages: forward problem and inverse problem. The first step is to solve a forward problem by measuring the capacitance of a region of interest. The capacitance is an ECVT response to the presence of a permittivity distribution. Capacitance values are measured based on the Poisson equation, which is integrated in three dimensions as follows:

$$C_i = \frac{1}{\Delta V_i} \oiint \varepsilon\left(x, y, z\right) \nabla \phi\left(x, y, z\right) \mathrm{d}A_i \tag{1}$$

where C_i is the measured capacitance of the ith pair between the electrode pair, ΔV_i is the voltage difference between the electrode pair, ε is the permittivity distribution, and ϕ is the potential distribution of the electric field.

The number of independent capacitance measurements depends on the number of sensors and the sensing method employed. If the number of sensor is n_e channels and if only one channel is activated iteratively as a Transmitter or a Receiver, then the number of independent measurements m is

$$m = 0.5 n_e (n_e - 1) \tag{2}$$

Another variation of the sensing method features the combination of multiple electrodes to apply an excitation signal to obtaining the parallel excitation field [12]. The methods used to measure capacitance and to sensing depend on the capabilities of the data acquisition system.

2.2. **Image reconstruction.** Furthermore, to solve the inverse problem, the capacitance data are reconstructed into an image that represents the permittivity distribution. Actually, the field distribution in the region of interest depends on the distribution of electric properties. The relationship between the permittivity distribution and capacitance takes the form of a nonlinear differential equation (see Equation (1)), which is why the technique is called soft-field tomography. Nevertheless, the equation can be solved using a linear approach.

This linear approach is also called hard-field tomography. In hard-field tomography, the field distribution in the region of interest is not dependent on the electric property

distribution. Therefore, by using a sensitivity matrix, it is possible to reconstruct the permittivity distribution. An image reconstruction algorithm based on linear approach will use the sensitivity matrix as the mapping of relative permittivity distribution in the region of interest.

A popular reconstruction method is linear back projection (LBP). However, this reconstruction technique experiences problems due to the ill-posed problem and the restricted number of capacitance measurements. Therefore, by decreasing the ill-posedness, Tikhonov regularisation is expected to enhance the accuracy of a reconstructed image [13].

Actually, this image reconstruction method is based on a single-step technique. To obtain a sharper reconstructed image, some studies have developed iterative image reconstruction techniques. One popular iterative image reconstruction technique that has been used widely in ECT and ECVT is iterative linear back projection (ILBP). ILBP is based on the iterative minimisation of the mean square error (MSE) objective function. Due to noise contamination and the iterative use of the least-square functions, ILBP produces so-called "sensitivity-caused artefacts" [9]. To overcome this issue, more than one objective function is required. Therefore, the NN-MOIRT image reconstruction technique is used, which features four objective functions: a negative entropy function, a least-squares error, a smoothness and small peakedness function, and a 3D-to-2D matching function.

3. **Sensor Designs and Sensitivity.** There are many issues related to sensor design [14]: the number and length of electrodes, the use of external and internal electrodes, various earthed screens, driven guard electrodes, high-temperature and pressure effects, twin-plane sensors and diameter limitations. In this study, sensors were designed by configuring the shapes of the electrodes. We analysed four geometries: rectangular, triangular, trapezoidal, hexagonal vertically aligned and hexagonal horizontally aligned (see Figure 2).

The sensors consisted of 32 channels and were arranged into four planes. The number of channels can be changed and adjusted according to the ability of the data acquisition system. All vessels have the same inner diameter of 11.4 cm.

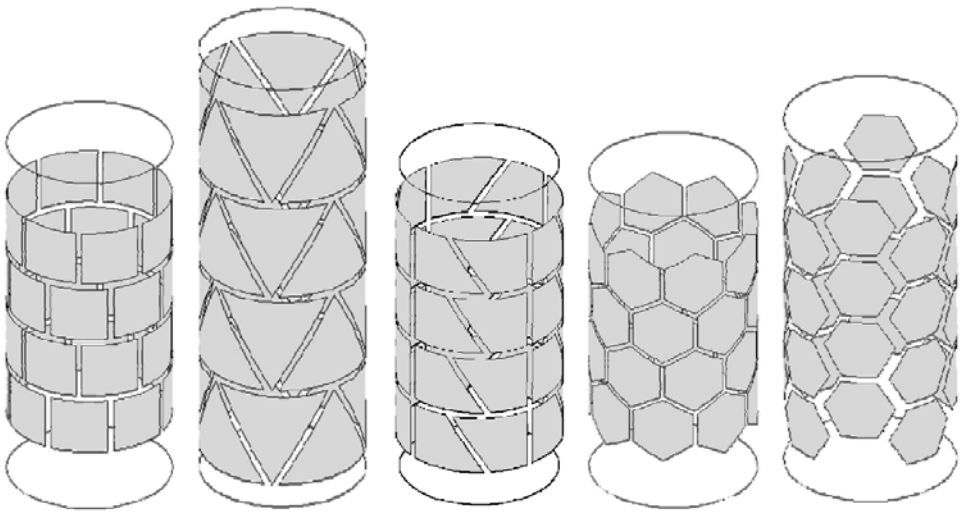

FIGURE 2. Sensor designs: (from left to right) rectangular shape, triangular shape, trapezoid shape, hexagonal vertically-aligned shape and hexagonal horizontal-aligned shape

To obtain a reconstructed image based on Equation (3), a sensitivity matrix S is required. The sensitivity matrix is the characteristic of the capacitance sensor, which had unique properties for each sensor because of the variation in electrode geometry. There are two methods to obtain the sensitivity of the sensor capacitance: the perturbation method [15] and the multiplication of electric field distribution [16]. In both methods the domain was split into several voxel imaging domains whose numbers are adjusted to the capabilities of the PC used. Increasing the number of voxels will increase the level of image resolution but will slow the reconstruction process because the memory required to generate the variable matrix will also increase dramatically. In this study x, y and z axes were divided into 32 pixels, so there were $32 \times 32 \times 32 = 32,768$ voxels.

The sensitivity of the sensor used in this study is approximated [16] by

$$S_{i,j} = \frac{\bar{E}_i(x,y,z) \cdot \bar{E}_j(x,y,z)}{V_i \cdot V_j} \quad i \neq j \tag{3}$$

where $S_{i,j}$ is the sensitivity of electrode pair i and j. E_i is the electric field distribution when only the electrode ith is activated with a voltage V_i, and E_j is the electric field distribution when only the electrode jth is activated with a voltage V_j.

4. **Experiment.** The study was carried out by experiment to reconstruct a sphere object (rubber ball and plastic ball filled with water) and a sloped-cut acrylic cylinder (see Figure 3). The sloped-cut cylinder had the same diameter as the inner diameter of the cylindrical vessel (11.4 cm), was cut along a 60° angle and was 20 cm tall. The diameters of the rubber ball and plastic ball filled with water were both 6.6 cm. All capacitance measurements in this study were obtained with an ECVT-DAS 2G Active Differentiator made by Edwar Technology Co., which is capable of capturing data at four frames/second (one frame = 496 independent measurement).

FIGURE 3. Objects used for experiment

5. **Results and Discussion.**

5.1. **Effect of different shape designs.** The effect of different sensor designs can be observed in Figures 4 and 5. Figure 4 explains the normalised sensitivity distributions in 3D space for pairs of measurements between the 9th-13th electrodes and 4th-32nd electrodes. This figure shows that the five sensor configurations vary with respect to sensitivity along the three dimensions. It is caused that the geometry of 3D capacitance

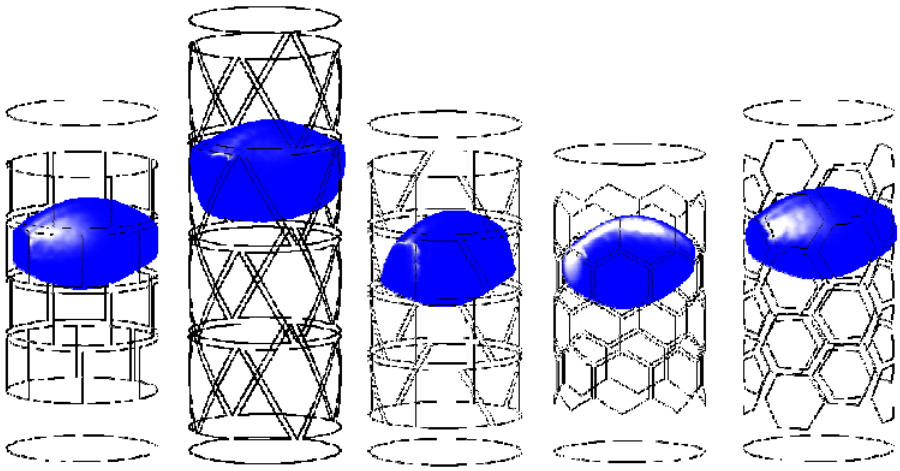

(a)

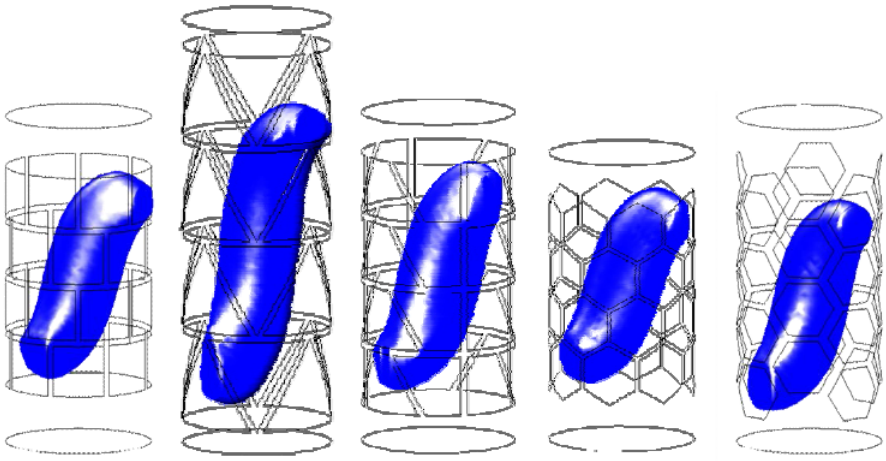

(b)

FIGURE 4. 3D sensitivity map of sensor design for pair measurement between (a) 9th-13th electrode and (b) 4th-32nd electrode

sensor affects the variation in the electric field distribution, not only along the radial direction but also along the axial direction.

Figure 5 shows the distribution of axial sensitivity for all sensors. The curves in the figure represent the sensitivity values of the 496 pairs of different measurement. Layers 1 to 32 were set up from the bottom to the upper layer of the vessels. It is showed that the axial sensitivity variation curves for the triangular and hexagonal-2 sensors (see Figure 5(b) and Figure 5(e)) are more homogeneous than those of other sensors exhibiting the same amplitude and width. The triangular sensor has an amplitude around 0.8, while that of the hexagonal-2 sensor is around 0.6. For the other sensors (see Figures 5(a), 5(c) and 5(d)), there are two types of curves with different widths and amplitudes. Figure 5 shows that the triangular and hexagonal-2 sensors show more variation in the sensitivity distribution along the axial direction than the other sensor geometries. According to [9], homogeneous sensitivity strength over the entire sensing domain is essential to avoid artefacts or image distortion in the reconstructed image. The factors that produce differences in the distribution of the electric field are the variation in the geometric centre of each sensor along the axial axis and the distances between these centres among adjacent

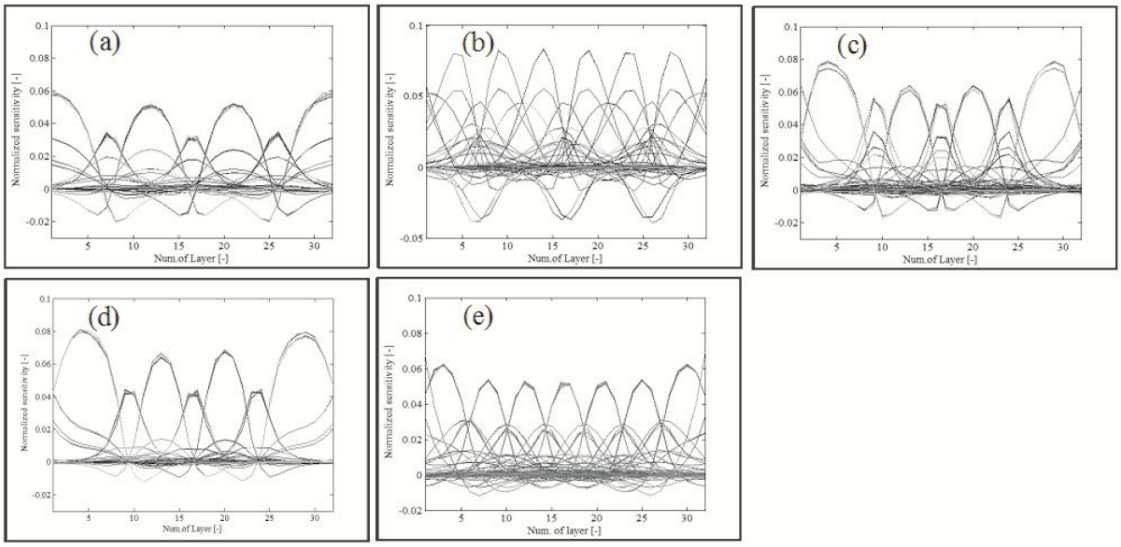

FIGURE 5. Axial sensitivity distribution for 496 independent measurements (a) rectangular, (b) triangular, (c) trapezoidal, (d) hexagonal-1 and (e) hexagonal-2 sensor

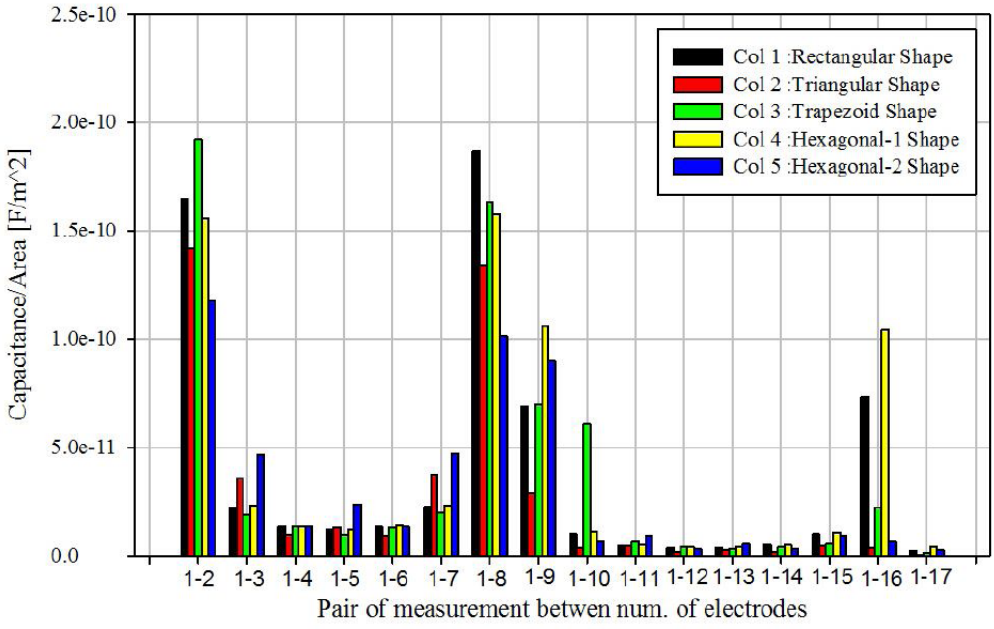

FIGURE 6. The comparison of capacitance data

sensors. The sensor with the greatest variation in its geometric centre along the axial direction was the hexagonal-2 sensor, which had as many as eight modes.

5.2. **Comparison of capacitance data.** Another effect of different shape designs is different capacitance data that will be acquired in each electrode even with the same medium, i.e., air ($\varepsilon = 1$). Figure 6 shows clearly the comparison of capacitance data from the first 16 measurements pair. It shows the variation of amplitude value from pair measurement between 1st-2nd electrode until 1st-17th electrode. In the same plane of measurement pairs, i.e., 1st-2nd until 1st-8th, only hexagonal-2 sensor has lower decreasing value in each pair measurement. Even the measurement with the different plane, i.e., 1st-9th, hexagonal-2 sensor also has lower decreasing value in each pair measurement.

It shows that hexagonal-2 sensor has the electrical field distribution in axial and radial direction more homogenous than other sensors.

5.3. **Image reconstruction performances.** Figure 7 shows the image reconstruction results for the plastic ball filled with water. The ball was placed in the middle of the vessel and was detected by five sensors (rectangular, triangular, trapezoidal, hexagonal-1

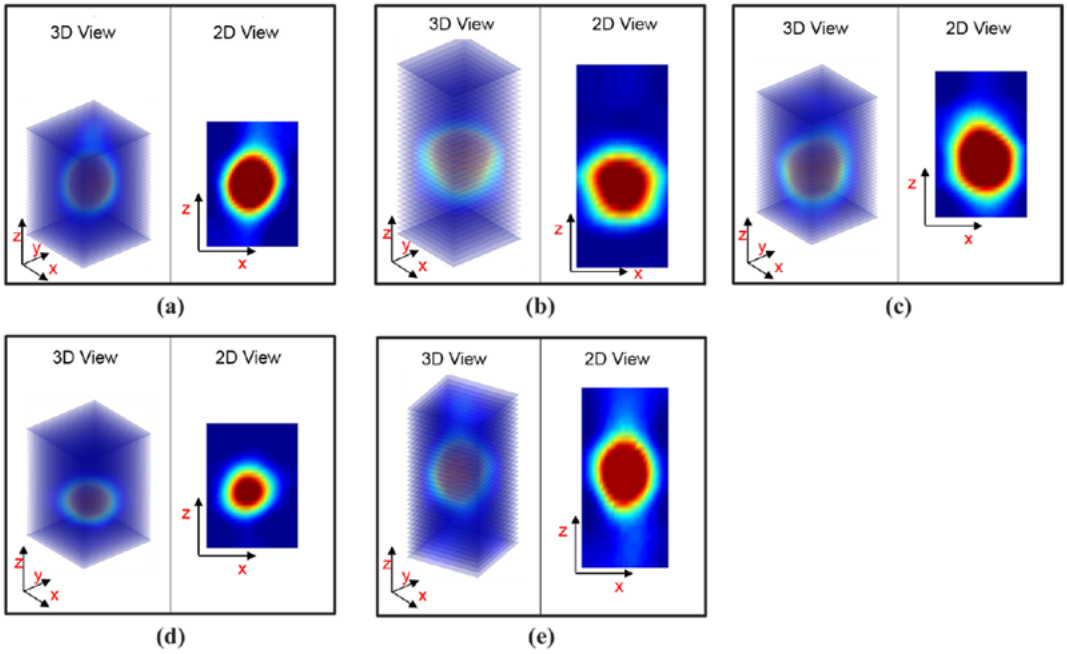

FIGURE 7. Image reconstruction results for the plastic ball filled with water: (a) rectangular, (b) triangular, (c) trapezoidal, (d) hexagonal-1 and (e) hexagonal-2 sensor

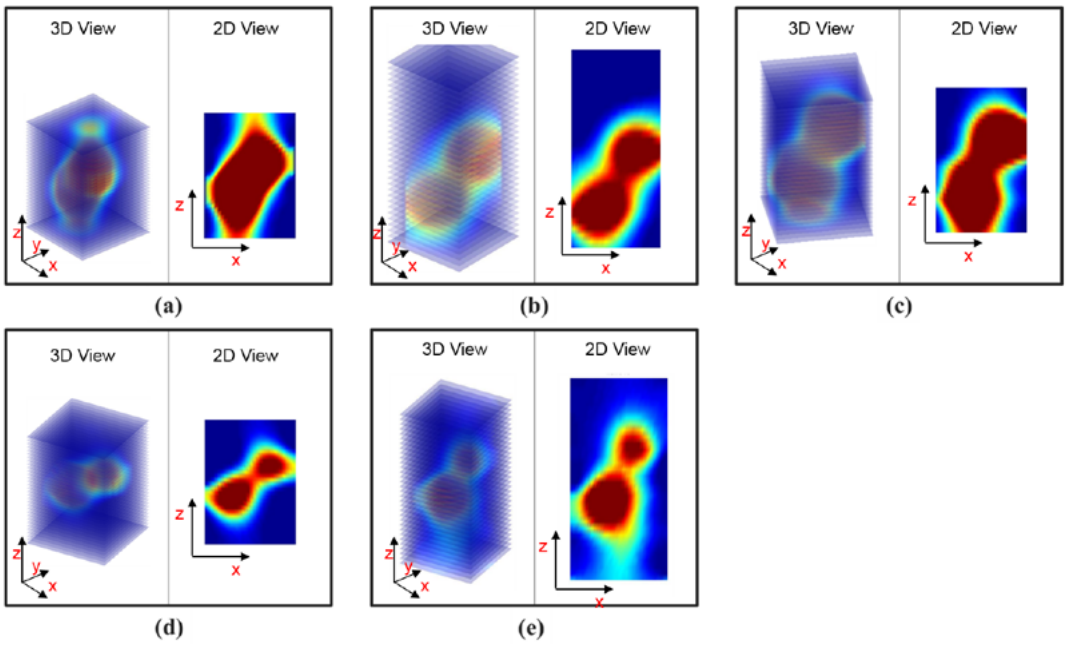

FIGURE 8. Image reconstruction results for rubber ball (upper) and plastic ball filled with water (lower): (a) rectangular, (b) triangular, (c) trapezoidal, (d) hexagonal-1 and (e) hexagonal-2 sensor

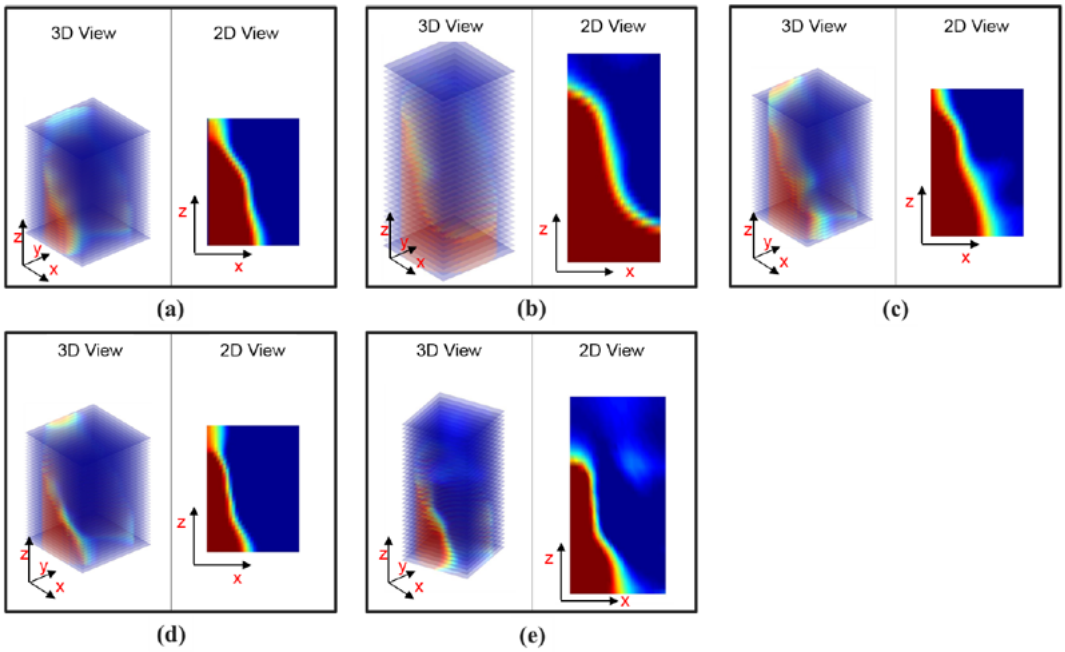

FIGURE 9. Image reconstruction results for sloped-cut acrylic cylinder: (a) rectangular, (b) triangular, (c) trapezoidal, (d) hexagonal-1 and (e) hexagonal-2 sensor

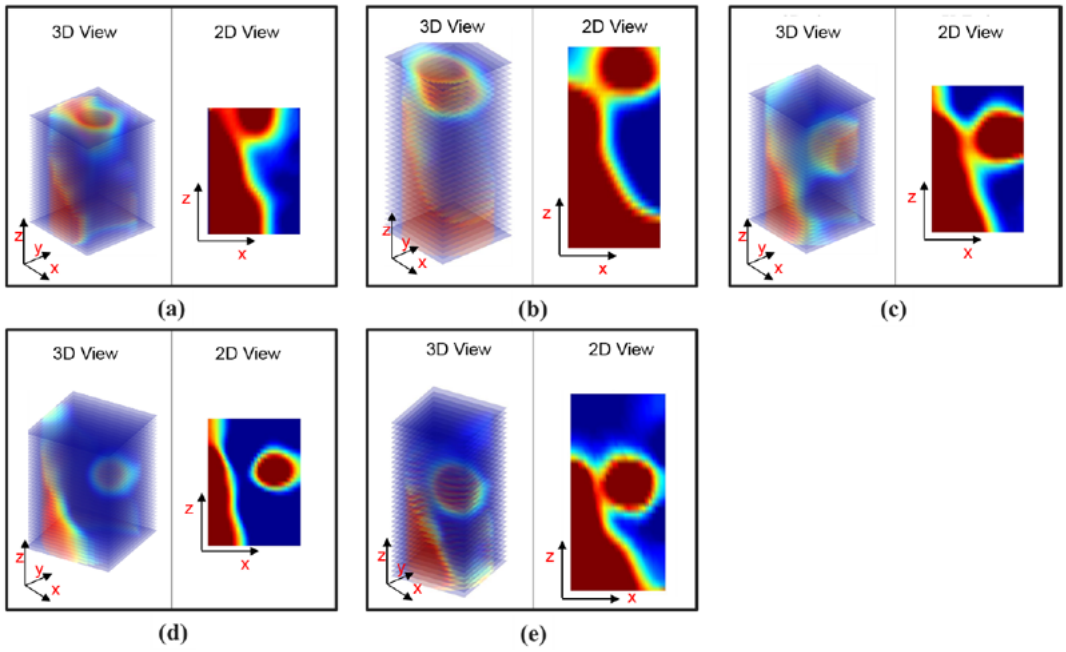

FIGURE 10. Image reconstruction results for sloped-cut acrylic cylinder and plastic ball filled with water: (a) rectangular, (b) triangular, (c) trapezoidal, (d) hexagonal-1 and (e) hexagonal-2 sensor

and hexagonal-2). However, the accuracy of the reconstructed image size was different between sensors. The hexagonal-1 sensor produced the smallest one. The evolutionary change in the accuracy of the reconstructed image of the object with respect to axial displacement was not monitored in this experiment; the object was simply placed in the middle of the vessel with respect to both the axial and radial directions.

Figure 8 shows the image reconstruction results for the rubber ball (upper) and plastic ball filled with water (lower). Both objects were placed in the middle of the axial direction and did not touch each other. It can be seen that the triangular, hexagonal-1 and hexagonal-2 sensors almost reconstructed the objects separately, while the rectangular and trapezoidal sensors failed to perceive the distance between the two objects.

Figure 9 shows the image reconstruction results for the sloped-cut acrylic cylinder. All sensors except the triangular sensor showed dead zones in the middle of the radial axis; this produced a cavity in the middle of the reconstructed object. However, this did not occur for the triangular sensor.

Figure 10 shows the image reconstruction results for the sloped-cut cylinder and water-filled plastic ball. The plastic ball was hung in the vessel but did not touch the sloped-cut acrylic cylinder. In this case, the hexagonal-1 sensor successfully imaged the objects separately; indeed, according to the results in Figure 10(c), this sensor showed a depression in the object image in the middle of the vessel along the radial direction.

6. **Conclusion.** In this study, the effects of electrode sensor shape (rectangular, triangular, hexagonal-1, trapezoidal and hexagonal-2) on the variations in the electric field distribution of an ECVT system were compared and analysed to obtain the optimal 3D sensor capacitance. The results concerning the axial sensitivity distribution indicate that the hexagonal-2 (hexagonal horizontally-aligned) and triangular sensors exhibit the greatest variation in the electric field distribution along the axial direction with uniform intensity. From the experiment, we can conclude that the reconstructed image of the hexagonal-2 shape sensor and triangular shape sensor are better in accuracy than the other sensors, even with rectangular shape sensor that popular and existed one in practical use.

Based on this study, the hexagonal-2 and triangular sensor are suitable for future application of ECVT. The configuration of sensor can be modified and mixed based on these shapes. However, this effort is one of many steps to attain the reconstructed image to be more accurate. Therefore, another development of other aspect in the ECVT system is still possible and required.

Acknowledgment. This research was supported by a research grant from the Ministry of Higher Education Malaysia (PRGS/1/12/TK03/UKM/02/1).

REFERENCES

[1] Q. Marashdeh, F. Wang, L. S. Fan and W. Warsito, Velocity measurement of multi-phase flows based on electrical capacitance volume tomography, *IEEE Sensors Conference*, pp.1017-1019, 2007.

[2] B. Du, Q. Marashdeh, W. Warsito, A.-H. A. Park and L. S. Fan, Development of electrical capacitance volume tomography (ECVT) and electrostatic tomography (EST) for 3D densitiy imaging of fluidized bed system, *The 12th International Conference on Fluidization – New Horizons in FLuidization Engineering*, pp.473-480, 2007.

[3] W. Warsito and L. S. Fan, ECT imaging of three-phase fluidized bed based on three-phase capacitance model, *Chemical Engineering Science*, vol.58, pp.823-832, 2003.

[4] B. Du, W. Warsito and L. S. Fan, ECT studies of gas-solid fluidized beds of different diameters, *Industrial and Engineering Chemistry Research*, vol.44, pp.5020-5030, 2005.

[5] W. Warsito and L. S. Fan, Dynamics of spiral bubble plume motion in the entrance region of bubble columns and three-phase fluidized beds using 3D ECT, *Chemical Engineering Science*, vol.60, pp.6073-6084, 2005.

[6] W. Warsito and L. S. Fan, Measurement of real-time flow structures in gas-liquid and gas-liquid-solid flow systems using electrical capacitance tomography (ECT), *Chemical Engineering Science*, vol.56, pp.6455-6462, 2001.

[7] M. Mukhlisin, A. Saputra, A. El-Shafie and M. R. Taha, Measurement of dynamic soil water content based on electrochemical capacitance tomography, *Int. J. Electrochem. Sci.*, vol.7, pp.5467-5483, 2012.

[8] F. Wang, Q. Marashdeh, L. S. Fan and W. Warsito, Electrical capacitance volume tomography: Design and applications, *Sensors*, vol.10, pp.1890-1917, 2010.

[9] W. Warsito, Q. Marashdeh and L. S. Fan, Electrical capacitance volume tomography, *Sensors*, vol.7, pp.525-535, 2007.

[10] Q. Marashdeh, W. Warsito and L. S. Fan, A volume tomography multimodal system based on ECT sensor, *The 5th World Congress on Industrial Process Tomography*, pp.1-6, 2007.

[11] Q. Marashdeh, L. S. Fan, B. Du and W. Warsito, Electrical capacitance tomography: A perspective, *Industrial and Engineering Chemistry Research*, vol.47, pp.3708-3719, 2008.

[12] W. Q. Yang, D. M. Spink, J. C. Gamio and M. S. Beck, Sensitivity distributions of capacitance tomography sensors with parallel field excitation, *Measurement Science and Technology*, vol.8, pp.562-569, 1997.

[13] L. H. Peng, H. Merkus and B. Scarlett, Using regularization methods for image reconstruction of electrical capacitance tomography, *Particle and Particle Systems Characterization*, vol.17, no.3, pp.96-104, 2000.

[14] W. Yang, Design of electrical capacitance tomography sensors, *Measurement Science and Technology*, vol.21, pp.1-13, 2010.

[15] Q. Marashdeh and F. L. Teixeira, Sensitivity matrix calculation for fast 3-D electrical capacitance tomography (ECT) of flow systems, *IEEE Transactions on Magnetics*, vol.40, pp.1204-1207, 2004.

[16] W. R. B. Lionheart, Reconstruction algorithms for permittivity and conductivity imaging, *The 2nd World Congress Industrial Process Tomography*, pp.4-11, 2001.